

# Effects of Diaphragm Spacing and Stiffness on the Dynamic Behavior of Curved Steel Bridges

E. M. Lui\*, Y. Liu<sup>1</sup> and M. Oguzmert<sup>2</sup>

*Chair, Department of Civil & Environmental Engineering, Syracuse University, Syracuse, NY 13244-1190, USA*

*<sup>1</sup>Structural Engineer, Hawk Engineering, PC, Binghamton, NY 13902, USA*

*<sup>2</sup>Graduate Assistant, Department of Civil & Environmental Engineering, Syracuse University, Syracuse, NY 13244-1190, USA*

---

## Abstract

This study investigates the curvature, diaphragm spacing, and diaphragm stiffness effects on the dynamic response of curved steel bridges. The bridges under investigation are simple-span non-skewed slab-on-girder bridges. The bridges are modeled using finite elements. The validity of the finite element models is established through comparison with theoretical and numerical solutions available in the literature. Eigenvalue and spectral analyses are carried out on one straight and three horizontally curved I-girder bridges with different values of diaphragm stiffness and diaphragm spacing. The results show that the dynamic response of these curved bridges is influenced more by their curvature than by the stiffness and spacing of the diaphragms. Although the effect of diaphragm spacing appears to be more pronounced for curved bridges with dominant in-plane bending and torsion modes, a response spectrum analysis has demonstrated that its effect on the internal forces and moments in the bridge members is only modest. Consequently, it can be concluded that in terms of dynamic behavior, diaphragm spacing and stiffness have little significance on the design of this type of bridges.

**Keywords:** curved bridge, diaphragm effect, dynamic behavior, finite element analysis

---

## 1. Introduction

For aesthetic consideration as well as simplicity in arrangement, details, and construction, the use of curved steel members has gained popularity for highway bridges located on horizontally curved alignments (Taly, 1998). In addition to aesthetics, the use of curved geometry has allowed bridge engineers to design bridges for greater span lengths and fewer piers. If straight girders are used along the chords of a curved bridge, large and unequal deck overhangs may occur that could lead to an uneven shadowing on the girders or result in an undesirable appearance. Curved members are also good candidates for satisfying the strict demand placed on highway structures by predetermined roadway alignments and tight geometric restrictions.

The dynamic responses of horizontally curved beams and bridges have been the subject of research by numerous investigators since the 1960s. Culver (1967) developed an exact solution for the equations of motion governing the free vibration response of a horizontally curved beam with two simply supported ends, and approximate solutions for horizontally curved beams with

fixed-fixed as well as fixed-simply supported end conditions. Tan and Shore (1968a) modeled a horizontally curved bridge as a curved beam and solved the governing differential equations for the free and forced vibrations of the beam to investigate its dynamic response to a constant moving load. They concluded that changing either the radius of curvature or the rigidity ratio would result in a change of the fundamental natural frequency of the horizontally curved bridge. In another study, Tan and Shore (1968b) derived and solved the differential equations governing the dynamic response of a horizontally curved bridge subjected to a forcing system consists of springs and masses that simulate a vehicle traveling on the bridge to investigate the effects of weight ratio and frequency ratio on the dynamic behavior of the bridge. Christiano and Culver (1969) formulated and solved the equations governing the dynamic behavior of a single span, horizontally curved bridge with an open cross-section to study the response of the bridge to a moving load. Shore and Chaudhuri (1972) solved the governing differential equations to investigate the effects of transverse shear deformation and the flexural rotatory inertia on the natural frequencies of a horizontally curved beam. Chaudhuri and Shore (1977) used the finite element method to study the dynamic response of horizontally curved I-girder bridges subjected to simulated highway loadings. In their bridge model, the deck was modeled

---

\*Corresponding author  
Tel: +315-443-3394  
E-mail: emlui@syr.edu

using annular plate elements, the girders were modeled by one-dimensional thin-walled circularly curved beam elements, and the transverse diaphragms were modeled using straight prismatic beam and frame elements. Yoo and Fehrenbach (1981) developed exact stiffness matrices for horizontally curved girders by utilizing the shape functions derived from the solutions of the homogeneous differential equations governing the static behavior of these girders, and solved the element relationships numerically to study the natural frequencies of these girders with different end conditions. Mukhopadhyay and Sheikh (1995) studied the large amplitude vibration of horizontally curved beams having varying included angles, radii, amplitude ratios and support conditions. Huang *et al.* (1995) modeled a horizontally curved bridge as a planar grillage beam system composed of horizontally curved beam elements and straight beam elements to investigate the dynamic behavior of curved I-girder bridges due to one or two trucks (placed side by side) moving across rough bridge decks and found that the impact factors of bending and shear for inside girders of curved I-girder bridges were significantly smaller than those for outside girders. Kawakami *et al.* (1995) developed an approximate method based on a combination of numerical integration and numerical solution of integral equations to analyze the free vibration of horizontally curved beams with arbitrary shapes and variable cross-sections. Kang *et al.* (1996) studied the free vibration response of horizontally curved single-span, wide-flange beams having a range of non-dimensional parameters representing variations in warping stiffness, torsional stiffness, radius of curvature, included angle of the curve, polar mass moment of inertia, and various end conditions by using differential quadrature method. More recently, Howson and Jemah (1999) developed exact dynamic stiffness from the governing differential equations of motion and studied the out-of-plane frequencies of curved Timoshenko beams. Huang *et al.* (1998) used a finite element model to study the dynamic response and impact characteristics of a series of thin-walled concrete box girder curved bridges subject to AASHTO HS20-44 truck load simulated as a multi-degree-of-freedom nonlinear vehicle model.

Although much work has been reported on the subject, most of the studies described in the foregoing apply only to curved beams. Except for the work reported by Maneetes and Linzell (2003) and a few others, the study of the dynamic behavior of curved bridges of which curved girders are a component has been scanty. In particular, very little work has been done to investigate the vibration response of horizontally curved steel bridges taking into consideration the combined influence of curvature, diaphragm spacing and diaphragm stiffness effects. At present, diaphragms and cross-frames are designed for static conditions only (Chen and Duan, 2000). In particular, the American Association of State Highway and Transportation Officials (AASHTO, 2004) specifies that diaphragms or cross-frames shall be

designed to ensure:

- Transfer of lateral wind loads from the bottom of the girder to the deck and from the deck to the bearings,
- Stability of the bottom flange for all loads when it is in compression,
- Stability of the top flange in compression prior to curing of the deck, and
- Distribution of vertical dead and live loads applied to the structure.

Because no guidelines are provided for the design of these diaphragms under dynamic or earthquake conditions, the main objective of the present study is to determine whether the inclusion of diaphragm effect in the dynamic analysis of curved bridges will produce results appreciable enough to warrant its inclusion in the seismic design of curved bridges.

The inclusion of diaphragm effect in a dynamic analysis undoubtedly complicates the problem. However, the associated mathematical difficulties can be overcome with the use of the finite element method (FEM) of analysis. The FEM is therefore used in the present study.

In the following section the effects of mass and stiffness changes on the free-vibration response of a structure is discussed. This is followed by a description of the finite element model used for the present investigation. Results of a series of numerical studies performed on a straight and three curved bridges are then presented and compared. Using spectral analysis, the seismic behavior of the four bridges with different numbers of diaphragms under three different earthquakes is described. Conclusions are made based on the results of these analyses.

## 2. Effects of Mass and Stiffness Changes

When there is a change in the mass and/or stiffness of a structure, its modal properties such as natural frequencies and mode shapes will change. In theory, the natural frequencies and mode shapes of the modified structure must satisfy an eigenvalue equation

$$[(\mathbf{K} + \Delta\mathbf{K}) - \omega_{im}^2(\mathbf{M} + \Delta\mathbf{M})]\phi_{im} = 0 \quad (1)$$

where  $\mathbf{K}$  and  $\mathbf{M}$  are the original system stiffness and mass matrices, respectively.  $\Delta\mathbf{K}$  and  $\Delta\mathbf{M}$  are the changes in stiffness and mass, respectively.  $\omega_{im}$  is the  $i$ th mode natural frequency corresponding to the  $i$ th mode shape  $\phi_{im}$  of the modified system.  $\omega_{im}$  and  $\phi_{im}$  are related to the original natural frequency  $\omega_i$  and mode shape  $\phi_i$  by the equations

$$\omega_{im} = \omega_i + \Delta\omega_i, \quad \phi_{im} = \phi_i + \Delta\phi_i \quad (2)$$

where  $\Delta\omega_i$  and  $\Delta\phi_i$  represent the change in the  $i$ th mode natural frequency and mode shape of the modified system.

The amount of perturbation in natural frequency and mode shape depends not only on the magnitude but also on the manner by which the mass and stiffness of the system are changed. As an example, consider the simply

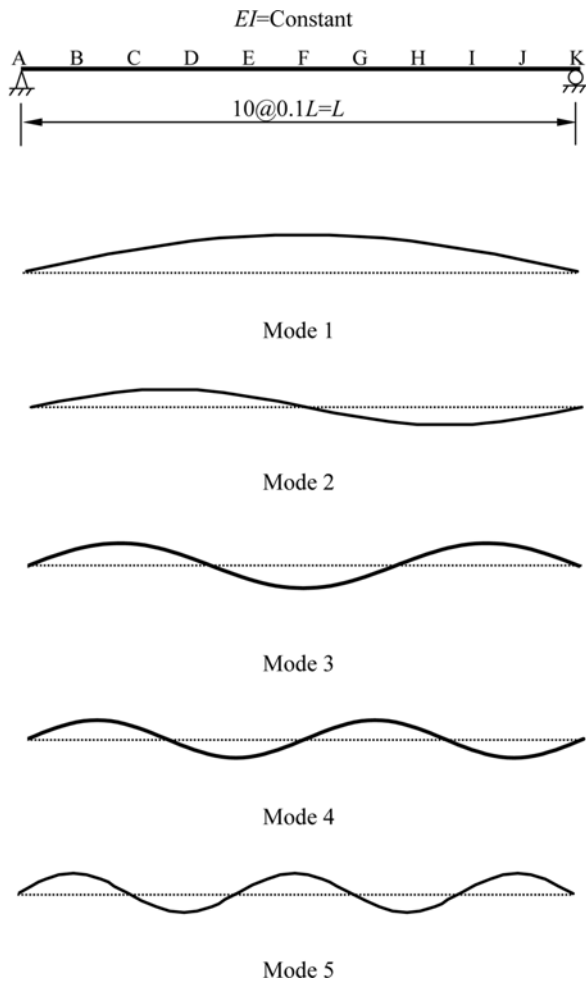


**Figure 1.** Free vibration response of a simply-supported beam.

supported beam shown in Fig. 1. If the flexural rigidity  $EI$ , density  $\rho$ , and cross-sectional area  $A$  are all constants along the length  $L$  of the beam, its natural frequencies for transverse vibration ignoring shear deformation effect are given by the equation

$$\omega_i = i^2 \pi^2 \sqrt{\frac{EI}{\rho AL^4}}, \quad i = 1, 2, \dots, n \quad (3)$$

The corresponding mode shapes (of which the first five are shown in Fig. 1) are given by

$$\phi_i = C \sin\left(\frac{i\pi}{L}x\right), \quad i = 1, 2, \dots, n \quad (4)$$

where  $C$  is a constant.

Suppose a mass equal to 10% of the mass of the beam is added to the system. Its effect on the natural frequencies of the beam is dependent on where the added mass is located. From Table 1 in which the percent changes in the first five natural frequencies are shown, it can be seen that the added mass affects a particular natural frequency the most when it is placed at location(s) of maximum displacement for the mode shape that corresponds to that natural frequency. Similarly, if one increases the stiffness (obtained by doubling the moment of inertia at selected segments) of the beam, it can be seen from Table 2 the particular natural frequency that will be most affected by the added stiffness is the one that corresponds to the mode shape with the highest curvature. Another phenomenon that can be readily observed from these tables is that added mass decreases the system frequencies, whereas added stiffness increases the system frequencies.

**Table 1.** Effect of added mass location on natural frequency

Mode	Percent change in natural frequency, $[(\omega_{im} - \omega_i)/\omega_i] \times 100\%$				
	10% mass added on beam segment				
	AB and JK	BC and IJ	CD and HI	DE and GH	EF and FG
1	-0.382	-2.10	-4.65	-7.07	-8.47
2	-1.32	-5.89	-8.36	-5.89	-1.32
3	-2.59	-7.55	-4.35	-1.17	-5.70
4	-3.78	-6.23	-1.69	-6.23	-3.78
5	-4.55	-4.11	-4.22	-4.34	-3.80

**Table 2.** Effect of added stiffness distribution on natural frequency

Mode	Percent change in natural frequency, $[(\omega_{im} - \omega_i)/\omega_i] \times 100\%$				
	100% stiffness increase in beam segment				
	AB and JK	BC and IJ	CD and HI	DE and GH	EF and FG
1	0.318	2.16	5.41	8.98	11.3
2	1.23	7.04	11.3	7.04	1.23
3	2.54	10.8	5.88	0.984	10.6
4	3.99	10.5	1.24	10.5	3.99
5	5.38	6.74	6.29	5.89	7.99

**Table 3.** Comparison of results for horizontally curved beams with different subtended angles and radii of curvatures (1 in. = 2.54 cm)

Subtended Angle (deg)	Radius of Curvature (in.)	Present (40 elements)	Culver		Shore and Chaudhuri	
		$\omega_1$ (rad/s)	$\omega_1$ (rad/s)	Percent error	$\omega_1$ (rad/s)	Percent error
10	1155.5	197.0	202.5	-2.8	203.3	-3.2
20	577.8	183.2	184.3	-0.6	186.3	-1.7
30	385.2	160.9	162.2	-0.8	164.7	-2.4
40	288.9	139.2	140.0	-0.6	142.8	-2.6
50	231.1	119.8	120.9	-0.9	122.8	-2.5
60	192.6	102.9	103.8	-0.9	105.2	-2.2
70	165.1	88.3	88.9	-0.7	90.0	-1.9
80	144.4	75.7	76.0	-0.4	76.8	-1.5
90	128.4	64.6	64.6	0	65.2	-0.9

When diaphragms or cross-frames are installed on a bridge, mass and stiffness will be added. It is the intent of this study to determine what effect these diaphragms may have on the dynamic and seismic responses of horizontally curved slab-on-girder steel bridges.

### 3. Finite Element Model

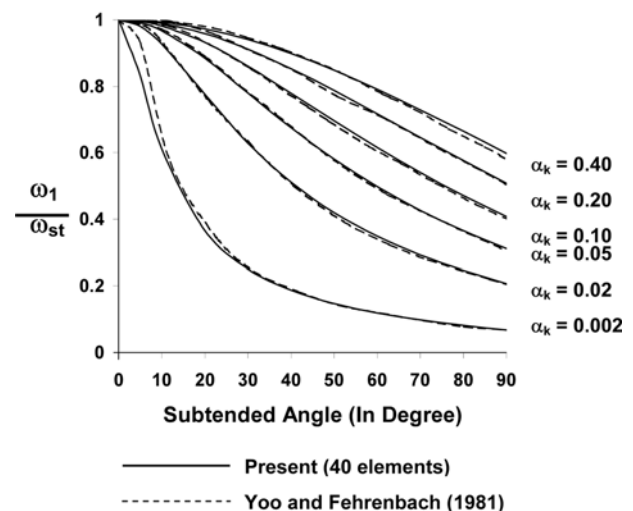
The software used for the present study is the general purpose finite element program ANSYS (2004). The steel girders and diaphragms were modeled using beam element, while the concrete deck was modeled using shell elements. A brief description of the model is given below.

#### 3.1. Modeling of the steel girders

In the present study, curved steel girders were modeled using a series of straight Beam188 elements. ANSYS's Beam188 element is a 3-D beam element suitable for analyzing slender to moderately short beam structures. Its formulation is based on the Timoshenko beam theory. The element has six and an optional seventh degrees of freedom per node. The six degrees of freedom are: translations in the x, y, and z directions; and rotations about the x, y, and z axes. The seventh degree of freedom, which can be activated or deactivated, allows the user to consider the effect of cross-section warping in the analysis. Based on a convergence study of a number of simply-supported curved beams with curvatures that vary from 0.002 to 0.01 ft<sup>-1</sup> (0.0066 to 0.033 m<sup>-1</sup>), it was determined that the optimal number of elements needed to obtain sufficiently accurate results was forty.

As an example, refer to Table 3 in which the fundamental frequencies  $\omega_1$  obtained using 40 elements are compared to those reported by Culver (1967), and Shore and Chaudhuri (1972) for a series of curved beams with different subtended angles and radii of curvatures. Good correlation is observed.

As another example, consider Fig. 2 in which results obtained using the present model is compared with those reported by Yoo and Fehrenbach (1981) on the fundamental frequencies of a series of simply-supported

**Figure 2.** Comparison of results for horizontally curved beams with different rigidity ratios.

curved beams with different rigidity ratios  $\alpha_k$  spread over a range of subtended angle from 10 to 90. The rigidity ratio  $\alpha_k = GK_T/EI_z$  (where  $G$  is the shear modulus,  $E$  is the modulus of elasticity,  $K_T$  is the torsional constant, and  $I_z$  is the moment of inertia about the strong axis of the cross-section) is defined as the ratio of torsional to flexural rigidity of the beam. The range of  $\alpha_k$  used varies from 0.002 to 0.4. According to Yoo and Fehrenbach, a rigidity ratio of 0.002 is roughly equivalent to that of an isolated wide-flanged beam, and a rigidity ratio of 0.4 is somewhat equal to that of a built-up deck section. In the figure all fundamental frequencies  $w_1$  are normalized by the corresponding fundamental frequencies of a straight beam  $\omega_{st}$  having the same material and cross-sectional properties, and curves are drawn between data points to show trends. It can be seen from the figure that good correlation is obtained between the two sets of results.

#### 3.2. Modeling of the concrete deck

The deck was modeled using Shell91 elements. ANSYS's Shell91 is an 8-node nonlinear multi-layered shell element

**Table 4.** Comparison of natural frequencies (radians/sec)

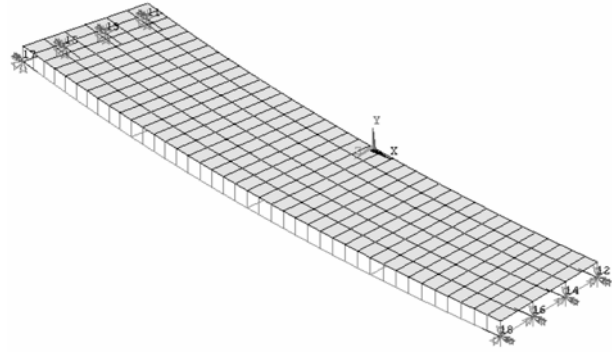
m n	1		2		3		4		5		6	
	Present	Theory										
1	37.3	37.4	43.2	43.5	53.3	53.7	67.3	67.9	85.5	86.3	107.7	108.7
2	143.0	143.5	148.9	149.6	158.8	159.8	172.6	174.1	190.0	192.4	212.0	214.8

that has six degrees of freedom per node: translation in the nodal x, y, z directions; and rotations about the nodal x, y, and z axes. To establish the optimal number of elements to be used, a convergence study was performed using various deck aspect (length-to-width) ratios. The study showed that the use of 240 elements would give good results for deck aspect ratios in the range of 2 to 10. This range of aspect ratios is considered inclusive of most slab-on-girder type bridge decks. As a representative example, Table 4 shows a comparison of the numerically obtained natural frequencies with their theoretical values given by Soedel (1981) for a simply-supported rectangular flat plate 100 ft. (30.5 m) long, 24 ft. (7.315 m.) wide, and 8 in. (20.3 cm) thick modeled using a 40×6 grid of elements. The material properties used were: elastic modulus  $E = 3,000$  ksi (20.7 GPa), Poisson ratio  $\nu = 0.16$ , and mass density  $\rho = 4.5$  slugs/ft<sup>3</sup> (2300 kg/m<sup>3</sup>). The values  $m$  and  $n$  correspond to the number of half sine waves along the long and short dimensions of the plate, respectively.

### 3.3. Modeling of the diaphragms

Diaphragms in the form of channel or W sections that connect adjacent parallel girders were modeled using Beam4 element. ANSYS's Beam4 element is a 3-D uniaxial element with tension, compression, torsion, and bending capabilities. The element has six degrees of freedom per node: translations in the x, y, and z directions; and rotations about the x, y, and z axes. Because diaphragms are often connected to the girders by connection plates that are welded to the girders, the model assumes that the connections between the diaphragms and the girders are rigid.

The composite action between the bridge deck and the supporting girders was modeled using massless rigid elements. Because the centroidal axes of the girders and the mid-surface of the deck do not lie on the same plane, these rigid elements are used to tie the centroids of the concrete deck and the steel girders together to simulate full composite action. The height of the rigid elements is taken as the vertical distance between the mid-surface of

**Figure 3.** A Horizontally curved bridge model.

the bridge deck and the centroidal axes of the girders. Figure 3 shows a typical ANSYS model of a horizontally curved bridge.

A curved bridge used in a paper by Huang *et al.* (1995) will be used to test the viability of the aforementioned modeling technique. The bridge in question has a centerline length of 100 ft. (30.5 m), a centerline radius of 500 ft. (152 m), and a superelevation  $e = 0.12$ . The bridge deck consists of a reinforced concrete bridge slab with a width of 27.28 ft. (8.315 m) and a thickness of 7.5 in. (19 cm) supported by four curved steel girders. The girders are connected transversely by seven equally spaced diaphragms. The cross-section properties and mass per unit length used for the different bridge components in the structural model are summarized in Table 5.

Because values for the warping constant were not reported by Huang *et al.* for the girders, it was assumed that the warping restraint effect was not considered in their analysis. As a result, the warping deformation option for Beam188 was turned off in the analysis.

The first six natural frequencies obtained using the present method are compared in Table 6 to those reported by Huang *et al.* obtained using the planar grillage beam model. The results are quite comparable. The slight discrepancy is likely due to the use of rather different approaches to model the bridge (finite element versus the grillage models).

**Table 5.** Bridge properties

Component	$I_z$ (cm <sup>4</sup> )	$I_y$ (cm <sup>4</sup> )	$K_T$ (cm <sup>4</sup> )	$A$ (cm <sup>2</sup> )	Mass (kg/m)
Exterior girder	$4.731 \times 10^6$	$1.366 \times 10^5$	$5.089 \times 10^4$	$2.430 \times 10^3$	1916
Interior girder	$4.895 \times 10^6$	$1.413 \times 10^5$	$5.810 \times 10^4$	$2.021 \times 10^3$	1593
End diaphragm	$0.268 \times 10^6$	$0.077 \times 10^5$	$2.729 \times 10^4$	$0.193 \times 10^3$	152
Interior diaphragm	$0.600 \times 10^6$	$0.173 \times 10^5$	$4.221 \times 10^4$	$0.236 \times 10^3$	186

**Table 6.** Comparison of natural frequencies (Hz)

Mode	1	2	3	4	5	6
Present	4.48	5.13	15.4	17.9	18.3	20.1
Huang <i>et al.</i>	3.62	4.83	14.5	16.6	19.6	23.8

### 4. Eigenvalue analysis

In this section an eigenvalue analysis will be carried out to determine how diaphragm spacing and stiffness may affect the free vibration response of simply-supported curved steel I-girder bridges. Some useful observations are made based on frequency and mode shape results generated from these free vibration analyses.

#### 4.1. Description of the bridges

One straight and three horizontally curved simple-span I-girder bridges are considered in the present study. All the bridges have the same centerline length  $L = 100$  ft. (30.5 m) and are simply supported at both ends (i.e.,  $u = v = w = \phi_x = 0$ ). The lines of supports at the ends of the curved bridges are oriented in the radial direction. The deck of the straight bridge has no superelevation, but those of the curved bridges have a constant superelevation of  $e = 0.1$ . The radius of curvature of the curved bridges varies from 400 ft (122 m) to 100 ft (30.5 m), resulting in a range of subtended angles that varies from 0.25 rad. to 1.0 rad. as shown in Fig. 4.

All the bridges used in the present study have a reinforced concrete deck supported by, and acted compositely with, four steel girders that are connected transversely by diaphragms. The four steel girders are curved in plane and evenly spaced at a distance of 8 ft. (2.44 m) along the width of the deck and have the following cross-sectional properties: cross-sectional area  $A = 70$  in<sup>2</sup> (452 cm<sup>2</sup>), major axis moment of inertia  $I_z = 46,213$  in<sup>4</sup> ( $1.92 \times 10^6$  cm<sup>4</sup>), minor axis moment of inertia  $I_y = 1,334$  in<sup>4</sup> ( $5.55 \times 10^4$  cm<sup>4</sup>), torsional constant  $K_T = 15.83$  in<sup>4</sup> (658.9 cm<sup>4</sup>), warping constant  $C_w = 1.20 \times 10^6$  in<sup>6</sup> ( $3.22 \times 10^8$  cm<sup>6</sup>), height  $h = 62$  in (158 cm). Three diaphragm spacing: 50 ft (15.2 m), 25

ft (7.62 cm) and 12.5 ft (3.81 m) are used, giving a span length to diaphragm spacing ratio of 2, 4, and 8, respectively. The number of diaphragms used is therefore 3, 5, and 9 for each case. For the bridge with 5 diaphragms, three different diaphragm sizes are used. They are: Case 1,  $A = 27.02$  in<sup>2</sup> (174 cm<sup>2</sup>),  $I_z = 5,860$  in<sup>4</sup> ( $2.44 \times 10^5$  cm<sup>4</sup>),  $I_y = 10$  in<sup>4</sup> (416 cm<sup>4</sup>),  $K_T = 11.5$  in<sup>4</sup> (478.7 cm<sup>4</sup>); Case 2,  $A = 38.21$  in<sup>2</sup> (247 cm<sup>2</sup>),  $I_z = 11,720$  in<sup>4</sup> ( $4.88 \times 10^5$  cm<sup>4</sup>),  $I_y = 20$  in<sup>4</sup> (832 cm<sup>4</sup>),  $K_T = 23$  in<sup>4</sup> (957.3 cm<sup>4</sup>); Case 3,  $A = 46.80$  in<sup>2</sup> (302 cm<sup>2</sup>),  $I_z = 17,580$  in<sup>4</sup> ( $7.32 \times 10^5$  cm<sup>4</sup>),  $I_y = 30$  in<sup>4</sup> ( $1.25 \times 10^3$  cm<sup>4</sup>),  $K_T = 34.5$  in<sup>4</sup> (1436 cm<sup>4</sup>). The reinforced concrete deck has a constant centerline length of  $L = 100$  ft. (30.5 m), a width of 24 ft. (7.32 m), and total thickness of 8 in. (20.3 cm). In order to take into consideration the reinforcing steel bars, the deck is modeled using a three-layer shell element. The three layers are: (1) a 0.9-in-thick concrete cover, (2) a 0.1-in-thick reinforcing steel, and (3) a 7-in-thick concrete. The thickness of the reinforcing steel layer is calculated using the concept of equivalent area (i.e., the area of the reinforcing steel layer used in the finite element model is set equal to the area of reinforcing steel bars used in the deck). The amount of reinforcing bars is calculated using 50% of the amount of balanced steel bars. The yielding strength of the steel used is  $f_y = 60$  ksi (414 MPa), and the compressive strength of the concrete used is  $f'_c = 4$  ksi (27.6 MPa). The material properties used for steel are: elastic modulus  $E = 29,000$  ksi (200 GN/m<sup>2</sup>), shear modulus  $G = 11,200$  ksi (77.3 GN/m<sup>2</sup>), and mass density  $\rho = 15.2$  slugs/ft<sup>3</sup> (7850 kg/m<sup>3</sup>). The material properties used for concrete are: elastic modulus  $E = 3,000$  ksi (20.7 GPa), shear modulus  $G = 1293$  ksi (8.92 GPa), and mass density  $\rho = 4.5$  slugs/ft<sup>3</sup> (2300 kg/m<sup>3</sup>). Figure 5 shows the plan views of the curved bridge models with three, five and

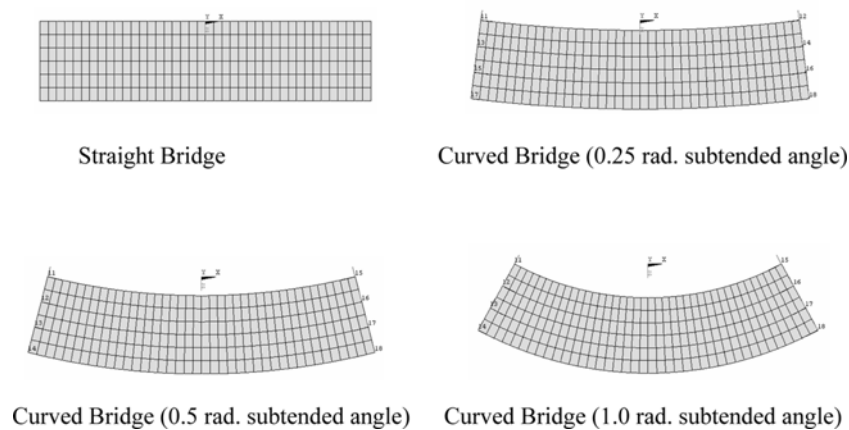


**Figure 4.** Plan view of bridges with different subtended angles.

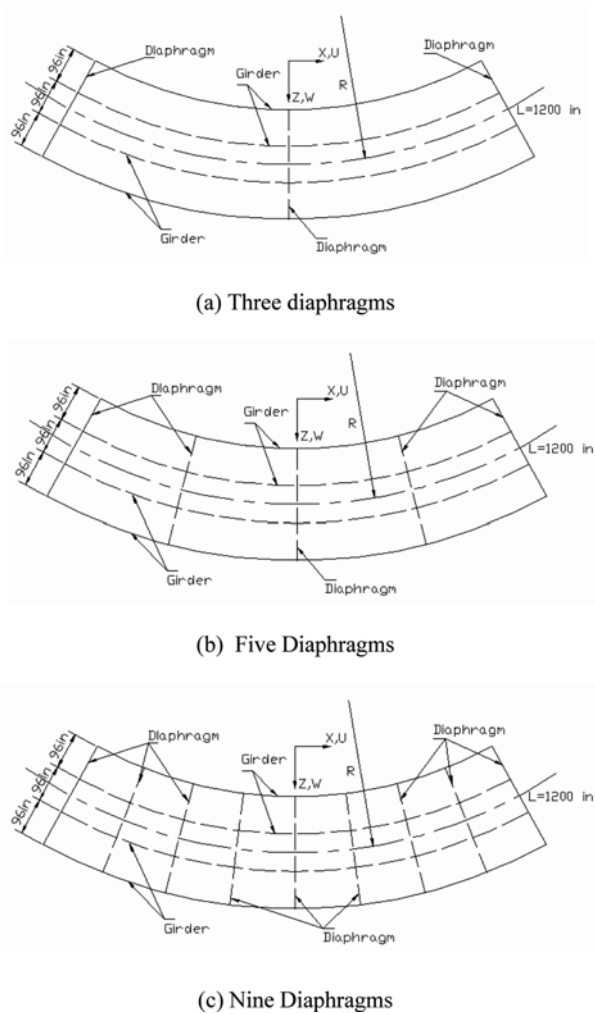


**Figure 5.** Plan view of curved bridges with different diaphragm spacing.

nine diaphragms, and Fig. 6 show the cross-section views of the straight and curved bridges.

**4.2. Effect of diaphragm spacing**

Using the aforementioned modeling technique, eigenvalue analyses were carried out for the bridges with different diaphragm spacing. The first eight natural frequencies for each bridge with 3, 5, and 9 diaphragms (i.e., with a span length to diaphragm spacing ratio of 2, 4 and 8) are summarized in Tables 7 to 10. Schematics of the first five mode shapes for the straight and curved bridges with five diaphragms are shown in Figs. 7 and 8, respectively. Based on the results of these analyses, the following conclusions can be made:

1. As expected, bending and torsional modes are always coupled for the curved bridges. The degree of coupling increases with the subtended angle.
2. Because the lower modes are often dominated by out-of-plane bending, and the higher modes are often dominated by torsion/twisting and in-plane bending, the increase in the number of diaphragms (which tends to increase the torsion/twisting and in-plane bending

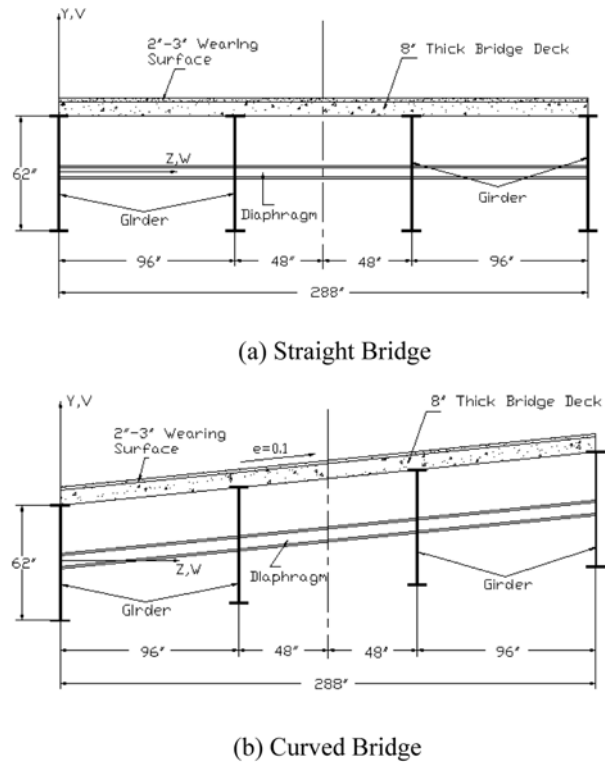


**Figure 6.** Straight and curved bridge cross-sections.

stiffness of the system) often results in an increase in the spread of frequencies, and hence increases the bandwidth of the frequency spectrum.

3. Increasing the number of diaphragms does not have much effect on the mode shape of the fundamental mode, but it does change the mode shapes for the higher modes (i.e., modes 2,3,4,5).

4. The high modes (i.e., modes 6,7,8) are almost exclusively bending and twisting of the girders between the diaphragms (i.e., they are local rather than global modes). Because diaphragms tend to restrain this type of girder deformation, the frequency increases somewhat with an increase in the number of diaphragms.

5. While for all the bridges the change in frequencies for the lower modes is almost negligible when the number of diaphragms is increased, the change becomes

**Table 7.** Natural frequencies (Hz) of a straight bridge with case 1 diaphragm stiffness and different diaphragm spacing

Mode	3-Diaphragm bridge	5-Diaphragm bridge	9-Diaphragm bridge
1	4.505	4.477	4.421
2	4.707	4.680	4.624
3	15.640	15.771	15.646
4	16.624	16.539	16.391
5	20.890	21.569	21.621
6	21.995	30.543	31.367
7	23.514	30.635	31.374
8	24.274	31.136	31.383

**Table 8.** Natural frequencies (Hz) of a curved bridge with case 1 diaphragm stiffness and different diaphragm spacing (Subtended angle = 0.25 rad.)

Mode	3-Diaphragm bridge	5-Diaphragm bridge	9-Diaphragm bridge
1	4.629	4.605	4.556
2	5.233	5.322	5.472
3	15.685	15.572	15.543
4	16.170	17.371	17.574
5	17.152	21.547	21.772
6	20.061	22.396	28.275
7	23.194	31.212	31.218
8	25.180	31.224	31.226

**Table 9.** Natural frequencies (Hz) of a curved bridge with case 1 diaphragm stiffness and different diaphragm spacing (Subtended angle = 0.5 rad.)

Mode	3-Diaphragm bridge	5-Diaphragm bridge	9-Diaphragm bridge
1	4.431	4.406	4.363
2	6.620	6.830	6.960
3	14.586	14.735	14.877
4	16.826	18.569	18.748
5	17.608	22.456	22.828
6	21.049	25.061	31.173
7	22.389	30.644	31.229
8	25.712	31.203	31.236

**Table 10.** Natural frequencies (Hz) of a curved bridge with case 1 diaphragm stiffness and different diaphragm spacing (Subtended angle = 1.0 rad.)

Mode	3-Diaphragm bridge	5-Diaphragm bridge	9-Diaphragm bridge
1	3.726	3.729	3.755
2	9.415	10.284	11.001
3	11.337	12.615	13.267
4	18.242	20.711	21.295
5	18.633	24.210	25.117
6	22.766	25.167	29.897
7	23.643	27.380	31.260
8	24.825	28.407	31.263

more noticeable for the higher modes, especially the high modes that involve local bending and twisting of the girders. Nevertheless, this change is more noticeable when the number of diaphragms is increased from 3 to 5, and less significant when the number of diaphragms is further increased to 9. This observation suggests that increasing the number of diaphragms beyond a span length to diaphragm spacing ratio of 4 will have a negligible effect on the dynamic response of the bridge.

**4.3. Effect of diaphragm stiffness**

In Tables 11 to 14, the first eight natural frequencies for

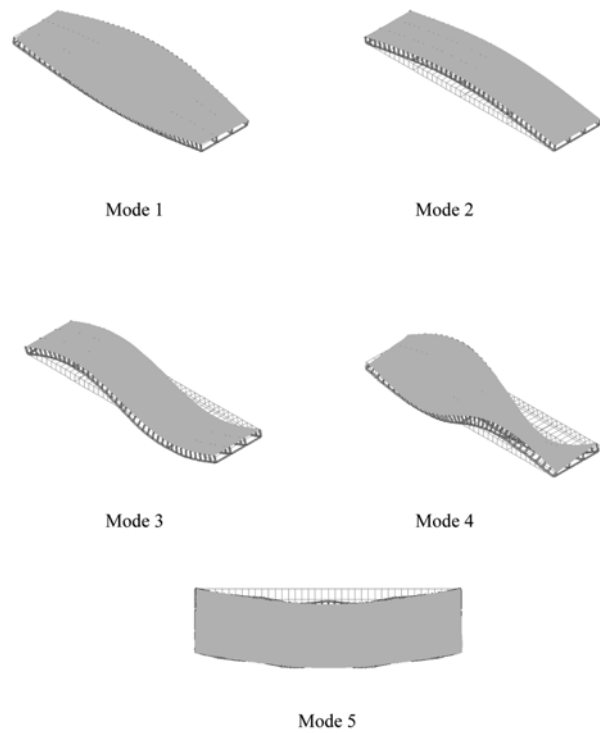


**Figure 7.** Natural vibration mode shapes (Straight bridge).

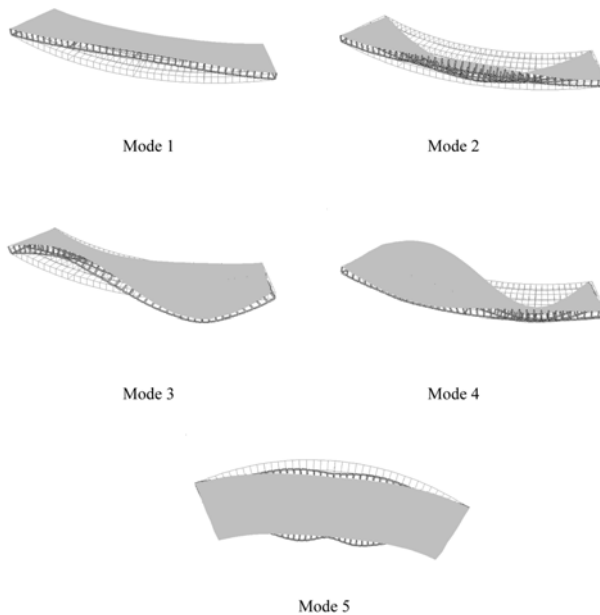


**Figure 8.** Natural vibration mode shapes (Curved bridge).

the four bridges with 5 diaphragms having different diaphragm stiffness labeled Case 1, 2 and 3 as described earlier are summarized. As can be seen, diaphragm stiffness changes the frequencies somewhat, but the change is quite minimal. It can therefore be concluded that diaphragm stiffness will not have a significant influence on the dynamic behavior of the bridges, regardless of whether it is straight or curved.

**Table 11.** Natural frequencies (Hz) of a straight bridge with 5 diaphragms and different diaphragm stiffness

Mode	Case 1 diaphragm	Case 2 diaphragm	Case 3 diaphragm
1	4.477	4.457	4.443
2	4.680	4.656	4.638
3	15.774	15.719	15.668
4	16.539	16.459	16.397
5	21.569	21.535	21.490
6	30.543	30.656	30.676
7	30.635	30.785	30.800
8	31.136	31.362	31.354

**Table 12.** Natural frequencies (Hz) of a curved bridge with 5 diaphragms and different diaphragm stiffness (Subtended angle = 0.25 rad.)

Mode	Case 1 diaphragm	Case 2 diaphragm	Case 3 diaphragm
1	4.605	4.582	4.564
2	5.322	5.307	5.291
3	15.572	15.510	15.457
4	17.371	17.317	17.263
5	21.547	21.577	21.550
6	22.396	23.627	24.541
7	31.212	31.184	31.153
8	31.224	31.212	31.201

**Table 13.** Natural frequencies (Hz) of a curved bridge with 5 diaphragms and different diaphragm stiffness (Subtended angle = 0.5 rad.)

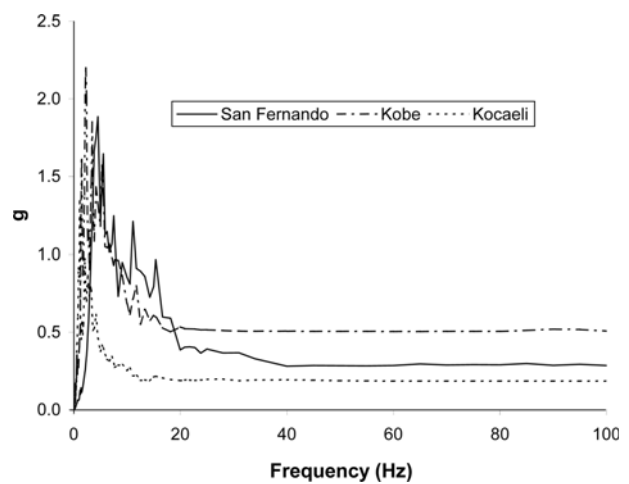
Mode	Case 1 diaphragm	Case 2 diaphragm	Case 3 diaphragm
1	4.406	4.384	4.368
2	6.829	6.812	6.792
3	14.735	4.701	14.659
4	18.569	18.556	18.522
5	22.456	22.469	22.435
6	25.061	26.902	28.091
7	30.644	30.908	30.870
8	31.203	31.203	31.206

## 5. Response Spectrum Analysis

The results of an eigenvalue analysis of the bridges discussed in the preceding section have demonstrated that the effects of diaphragm stiffness and spacing on the

**Table 14.** Natural frequencies (Hz) of a curved bridge with 5 diaphragms and different diaphragm stiffness (Subtended angle = 1.0 rad.)

Mode	Case 1 diaphragm	Case 2 diaphragm	Case 3 diaphragm
1	3.729	3.714	3.703
2	10.284	10.304	10.297
3	12.615	12.662	12.668
4	20.711	20.777	20.777
5	24.210	24.180	24.125
6	25.167	25.691	25.945
7	27.380	28.035	28.431
8	28.407	29.812	30.363

**Figure 9.** Earthquake response spectra.

natural frequencies of the bridges are not very pronounced. An explanation for this is that an increase in system stiffness is accompanied by a corresponding increase in mass when larger-sized and closer-spaced diaphragms are used for the bridges. In this section, results of a response spectrum analysis carried out for three earthquakes - San Fernando, Kobe and Kocaeli - will be presented to evaluate the effect of diaphragm stiffness and spacing on the seismic response of these bridges. These three earthquakes were selected because they exhibited different magnitudes, duration, and frequency contents to cover sufficient variability of strong ground motions to conduct response spectrum analyses and base conclusions on. The response spectra of the three representative earthquakes used in the present study are shown in Fig. 9 and pertinent characteristics of the each earthquake are summarized in Table 15.

**Table 15.** Earthquake characteristics

Earthquake	Location/Year	Station	Richter scale	Peak ground acceleration	Approx. duration
San Fernando	Sylmar-San Fernando, California, USA	Lake Hughes #12	6.6	0.283g	8 sec.
Kobe	Kobe, Japan	Nishi-Akashi	7.2	0.503g	20 sec.
Kocaeli	Kocaeli, Turkey	Arcelik	7.4	0.149g	45 sec.

**Table 16.** Results of response spectrum analysis (San Fernando Earthquake) (1 kip = 4.45 kN, 1 k-ft = 1.36 kN-m)

Bridge type	Number of diaphragms	Strong axis shear (kips)	Weak axis shear (kips)	Strong axis moment (k-ft)	Weak axis moment (k-ft)	Torque (k-ft)
Straight	3	5.24	97.9	471.5	14.8	0.247
	5	4.61	99.7	457.0	15.6	0.248
	9	3.19	102.8	430.4	9.85	0.248
Curved with 0.25 rad. Subtended angle	3	18.9	101.4	515.6	43.6	0.249
	5	18.9	98.3	502.7	44.3	0.254
	9	18.8	98.9	498.0	43.0	0.276
Curved with 0.50 rad. Subtended angle	3	11.7	108.9	615.0	15.7	0.221
	5	11.9	110.3	612.8	16.6	0.217
	9	11.6	113.6	616.1	17.2	0.227
Curved with 1.0 rad. Subtended angle	3	31.4	121.4	959.8	79.9	0.365
	5	33.4	117.8	976.1	83.3	0.441
	9	32.3	119.5	1047.9	62.2	0.263

**Table 17.** Results of response spectrum analysis (Kobe Earthquake) (1 kip = 4.45 kN, 1 k-ft = 1.36 kN-m)

Bridge type	Number of diaphragms	Strong axis shear (kips)	Weak axis shear (kips)	Strong axis moment (k-ft)	Weak axis moment (k-ft)	Torque (k-ft)
Straight	3	5.32	91.0	566.9	12.7	0.196
	5	4.70	88.9	547.3	13.9	0.197
	9	3.30	91.5	531.3	8.05	0.198
Curved with 0.25 rad. Subtended angle	3	19.2	95.8	597.2	44.7	0.249
	5	19.1	93.1	581.9	44.8	0.252
	9	18.7	94.0	574.3	42.1	0.272
Curved with 0.50 rad. Subtended angle	3	10.7	101.3	719.6	18.9	0.207
	5	10.9	102.4	722.7	20.1	0.202
	9	10.6	105.9	736.4	16.3	0.214
Curved with 1.0 rad. Subtended angle	3	33.0	124.4	899.0	74.5	0.378
	5	35.0	112.6	916.6	77.7	0.462
	9	33.9	124.7	982.2	58.2	0.271

**Table 18.** Results of response spectrum analysis (Kocaeli Earthquake) (1 kip = 4.45 kN, 1 k-ft = 1.36 kN-m)

Bridge type	Number of diaphragms	Strong axis shear (kips)	Weak axis shear (kips)	Strong axis moment (k-ft)	Weak axis moment (k-ft)	Torque (k-ft)
Straight	3	4.30	75.1	754.8	13.4	0.110
	5	3.77	69.6	738.2	11.3	0.107
	9	3.85	71.4	732.5	6.47	0.104
Curved with 0.25 rad. Subtended angle	3	10.0	79.1	818.4	18.0	0.150
	5	10.1	76.2	806.2	17.0	0.149
	9	10.3	77.1	802.9	14.9	0.161
Curved with 0.50 rad. Subtended angle	3	9.15	87.4	861.1	24.3	0.166
	5	9.44	89.4	859.0	24.5	0.169
	9	9.37	92.8	861.6	21.8	0.168
Curved with 1.0 rad. Subtended angle	3	28.5	107.0	1083.6	90.3	0.322
	5	30.3	106.5	1100.2	94.1	0.396
	9	29.3	107.3	1177.4	69.9	0.231

Using the Multimode Spectral Method of analysis for earthquake loads (AASHTO, 2004) in conjunction with the 100/30 rule for earthquake directional combinations and the Complete Quadratic Combination (CQC) rule for

modal combinations (Chen and Scawthorn, 2003), the absolute value of the maximum girder shears, moments and torques were calculated. The number of modes used in the analyses was such that the modal mass participation

exceeded 90% of the total mass of the structure (UBC, 1997; IBC, 2000) in the direction of ground motion. This resulted in a number that exceeded the AASHTO requirement that the number of modes used must be at least three times the number of spans for the bridge. The results so obtained are presented in Tables 16 to 18 for the three earthquakes. It can be seen in the tables that for a given bridge curvature, the maximum shear, moment and torque do not vary significantly. The maximum variation is within 10%. This variation is well within the amount of error expected in a response spectrum analysis. In addition, when an actual design is performed, a design (rather than the actual earthquake) spectrum is used. The averaging technique used in constructing the design spectrum will undoubtedly further reduce the amount of variability in the internal forces and moments. In the context of design for dynamic response, the sizing of the members will not be affected by the number and spacing of diaphragms.

While the effects of diaphragm stiffness and spacing are not significant, the results in the tables do indicate a strong dependence of the internal forces and moments on the amount of curvature of the bridge. Bridges with sharp curvatures often exhibit higher internal forces and moments.

## 6. Summary and Conclusions

The major objective of this paper is to investigate the effects of diaphragm stiffness and spacing on the dynamic behavior of simple-span non-skewed curved I-girder bridges. A finite element model of a curved bridge superstructure was developed, verified and used in a parametric study to evaluate the dynamic response of a series of straight and curved simple-supported bridges with different diaphragm spacing and stiffness. Based on this study, the following conclusions can be made:

1. Bending and torsion modes are always coupled for curved bridges.
2. While out-of-plane bending modes often dominate at low frequencies, torsion/twisting and in-plane bending modes usually dominate at higher frequencies. Beyond the first five modes, the mode shapes change from global to local with bending and twisting of girders occurring between diaphragms.
3. Diaphragm stiffness does not appear to have an appreciable effect on the frequencies and mode shapes of the curved bridges used in this study.
4. The effect of diaphragm spacing is more pronounced for curved bridges when compared to straight bridges. Decreasing the diaphragm spacing tends to increase the natural frequencies. However, this increase becomes insignificant when the bridge span to diaphragm spacing ratio exceeds 4.
5. Because the effects of diaphragm stiffness and spacing on the natural frequencies of the bridges are not appreciable, the variation of internal forces and moments obtained from a response spectrum analysis for curved

bridges with different diaphragm stiffness and spacing but with a given curvature are not substantial either.

6. While diaphragm stiffness and spacing have only modest influence on the dynamic response of curved bridges, the curvature of the bridge has a rather pronounced effect. Internal forces and moments increased noticeably for curved bridges with sharp curvatures.

## Acknowledgment

The authors would like to thank the reviewers and editors for their thorough reviews of this paper. Their valuable comments and constructive critiques have helped clarify certain aspects and enrich the general contents of this paper.

## References

- AASHTO (2004). *LRFD Bridge Design Specifications*, 3<sup>rd</sup> edition, American Association of State Highway and Transportation Officials, Washington, D.C.
- ANSYS (2004) Version 9, ANSYS, Inc. (www.ansys.com), Canonsburg, PA.
- Chaudhuri, S. K. and Shore, S. (1977). Dynamic Analysis of Horizontally Curved I-Stringer Bridges, *Journal of the Structural Division*, 103(ST8), pp. 1589-1604.
- Chen, W.F. and Duan, L., editors. (2000) *Bridge Engineering Handbook*, CRC Press, Boca Raton, FL.
- Chen, W.F. and Scawthorn, C., editors. (2003) *Earthquake Engineering Handbook*, CRC Press, Boca Raton, FL.
- Christiano, P. P. and Culver, C. G., (1969). Horizontally Curved Bridges Subject to Moving Load, *Journal of the Structural Division*, 95(ST8), pp. 1615-1643.
- Culver, C. G. (1967). Natural Frequencies of Horizontally Curved Beams, *Journal of the Structural Division*, ASCE, 93(ST2), pp. 189-203.
- Howson, W. P. and Jemah, A. K. (1999). Exact Out-of-Plane Natural Frequencies of Curved Timoshenko Beams, *Journal of Engineering Mechanics*, 125(1), pp. 19-25.
- Huang, D., Wang, T.-L., and Shahawy, M. (1995). Dynamic Behavior of Horizontally Curved I-Stringer Bridges, *Computers & Structures*, 57(4), pp. 703-714.
- Huang, D., Wang, T.-L., and Shahawy, M. (1998). Vibration of Horizontally Curved Box Stringer Bridges due to Vehicles", *Computers & Structures*, 68, pp. 513-528.
- IBC (2000). International Building Code, International Code Council, Falls Church, VA.
- Kang, K., Bert, C.W., and Striz, A.G. (1996). Vibration Analysis of Horizontally Curved Beams with Warping Using DQM, *Journal of Structural Engineering*, ASCE, 122(6), pp. 657-662.
- Kawakami, M., Sakiyama, T., Matsuda, H., and Morita, N. (1995). In-Plane and Out-of-Plane Free Vibrations of Curved Beams with Variable Sections, *Journal of Sound and Vibration*, 187(3), pp. 381-401.
- Maneetes, H. and Linzell, D.G. (2003). Cross-frame and Lateral Bracing Influence on Curved Steel Bridge Free Vibration Response, *Journal of Constructional Steel Research*, 59, pp. 1101-1117.
- Mukhopadhyay, M. and Sheikh, A. H. (1995). Large

- Amplitude Vibration of Horizontally Curved Beams: A Finite Element Approach, *Journal of Sound and Vibration*, 180(2), pp. 239-251.
- Shore, S. and Chaudhuri, S. (1972). Free Vibration of Horizontally Curved Beams, *Journal of the Structural Division*, 98(ST3), pp. 793-796.
- Soedel, W. (1981). *Vibrations of Shells and Plates*, Marcel Dekker, New York.
- Taly, N. (1998). *Design of Modern Highway Bridges*, McGraw-Hill, New York, NY.
- Tan, C. P. and Shore, S. S. (1968a). Dynamic Response of a Horizontally Curved Bridge, *Journal of the Structural Division*, 94(ST3), pp. 761-781.
- Tan, C. P. and Shore, S. S. (1968b). Response of a Horizontally Curved Bridge to Moving Load, *Journal of the Structural Division*, 94(ST9), pp. 2135-2151.
- UBC (1997). Uniform Building Code, Volume 2, *Structural Engineering Design Provisions*, International Conference of Building Officials, Whittier, CA.
- Yoo, C. H. and Fehrenbach, J. P. (1981). Natural Frequencies of Curved Stringers, *Journal of the Engineering Mechanics Division*, ASCE, 107(EM2), pp. 339-354.